Optik 127 (2016) 5852–5859

Contents lists available at ScienceDirect

Optik

journal homepage: www.elsevier.de/ijleo

A novel highly efficient algorithm for laser speckle imaging

Ping Kong, Yan-li Zhou, Yin-yue Xie, Meng Jiang*

School of Art and Science, Shanghai University of Medicine and Health Science, Shanghai 201318, China

ARTICLE INFO

Article history:
Received 23 November 2015
Accepted 6 April 2016

Keywords:
Laser speckle imaging
Speckle contrast
Background noise

ABSTRACT

Laser speckle imaging (LSI) is a non-invasive optical imaging technique able to provide wide-field two-dimensional maps of blood flow. The observer can either define different sizes for the region of interest to reduce the spatial variability or different time duration over which the blood flow values are averaged to decrease temporal variability. In this paper, we present a new algorithm for integrated speckle contrast, which accounts not only for temporal integration but for spatial integration as well, using a low time – consuming efficient algorithm. As a result, we find that an efficiency factor should be introduced to the measured speckle contrast to properly normalize and eliminate background noise; otherwise, the measured contrast is affected. Furthermore, we demonstrate its feasibility for relative flow speed assessing.

© 2016 Elsevier GmbH. All rights reserved.

1. Introduction

Laser speckle imaging (LSI) is a real-time, wide-field optical technique that can be used to visualize and monitor dynamic of blood flow changes in tissue. Since Fercher and Briers [1] extracted blood-flow information from the imaged speckle patterns in 1981, researchers have rapidly integrated LSI in their studies, which cover a wide range of applications, including ophthalmology, dermatology, dentistry, and neurobiology, among others [2]. In general imaging algorithms are either respectively based on temporal or spatial integration. The spatial algorithms are limited by its low resolution [3,4]. Although a higher spatial resolution can be obtained by means of the temporal algorithm, it can be only achieved under the precondition of high system complexity [4]. Thus, disadvantages of these algorithms limited applicability of the LSI technique. In order to solve this problem, Rege et al. have performed the experiment of LSI using a combination of the temporal and spatial algorithms [4]. This algorithm has a great advantage against others, except for background noise which is a big issue in the experiment. The same problem was encountered in Parthasarathy's research [5]. It is important to minimize or even completely reduce the noise, since the background noise makes a great impact on image contrast. On the other hand, due to the heavy computation burden of the image processing, some algorithms have been provided to improve the efficiency without any approximations such as Sums, FFT, and Roll Algorithm [6], and different irregular slide windows [7]. However, these irregular windows algorithms simply can be used only to certain shape of flow region [8]. Therefore, this algorithm cannot be applied to the whole flow region.

In this paper, we present a new algorithm expression for integrated speckle contrast which takes spatial and temporal variation into consideration. By decreasing the complexity of computational formula, high efficiency and short processing time can be achieved. Additionally, the system static contrast can be calculated using this new algorithm. This part of image contrast was conduct by background noise, and our target is to normalize and eliminate it for different systems. Finally, we

* Corresponding author.
E-mail address: jm_678@aliyun.com (M. Jiang).

http://dx.doi.org/10.1016/j.ijleo.2016.04.004
0030-4026/© 2016 Elsevier GmbH. All rights reserved.

demonstrate its potential advantage in relative flow speed evaluation. The experiment results show that our new algorithm has a great accuracy for wide band of flow speed.

2. Theoretical background and experimentation

2.1. Laser speckle imaging

Laser speckle is a random interference pattern produced by the coherent addition of scattered laser light with slightly different path lengths [9,10]. Motion of these scattering particles causes spatial and temporal modifications of the speckle pattern, either of which can be used to detect the speed of the scatterers. In the spatial domain, these modifications manifest themselves as localized blurring of the image. Laser speckle contrast imaging quantifies the extent of this localized spatial blurring by calculating a quantity called speckle contrast (K) over a small window (usually 7×7 pixels) of the image.

$$K = \frac{\sigma}{\langle I \rangle} \tag{1}$$

where σ is the standard deviation and I is the average intensity of the pixels of the window. For slower speeds, the pixels decorrelate less and hence K is large and vice versa.

The temporal fluctuations of speckles can be quantified using the electric field autocorrelation function $g_1(\tau)$. Typically$g_1(\tau)$is difficult to measure and the intensity autocorrelation function $g_2(\tau)$ is recorded. The field and intensity autocorrelation functions are related through the so-called Siegert relation.

$$g_2(\tau) = 1 + \beta |g_1(\tau)|^2 \tag{2}$$

where ß is a normalization factor which accounts for speckle averaging due to mismatch of speckle size and detector size, polarization and coherence effects. This effect has to be estimated by experiments. Recently, Bandyopadhyay et al. [11,12] used triangular weighting of the autocorrelation function to develop a more rigorous model relating speckle contrast to the correlation time, τ_c:

$$K(T, \tau_c) = \beta^{\frac{1}{2}} \left[\frac{e^{-2x} + 2x - 1}{2x^2} \right]^{\frac{1}{2}} \tag{3}$$

where $x = T/\tau_c$, T is the exposure duration of the camera. One disadvantage of these models is that they breakdown in the presence of scattered light. This can be corrected by modeling the scattered field, $E_h(t)$, as:

$$E_h(t) = E(t) + E_s e^{-iw_0 t} \tag{4}$$

where$E(t)$ is the Gaussian fluctuation, E_s is the static field amplitude and $w_0$is the source frequency. Eq. (2) can now be modified as:

$$g_2^h(\tau) = 1 + \frac{\beta}{(I_f + I_s)^2} \left[I_f^2 |g_1(\tau)|^2 + 2I_f I_s |g_1(\tau)| \right] = 1 + A\beta |g_1(\tau)|^2 B\beta |g_1(\tau)|$$

where $A = I_f^2/(I_f + I_s)^2$, and $B = 2I_f I_s/(I_f + I_s)^2$, $I_s = E_S E_S^*$ represents contribution from the static scattered light, $I_f = EE^*$ represents contribution from the dynamically scattered light. The second moment of intensity can be written using the modified Siegert relation as [11]:

$$I^2{}_T = \frac{\int_0^T \int_0^T I_i(t') I_i(t'') dt' dt''}{T^2}_i = I^2 \int_0^T \int_0^T \left[1 + A\beta \left(g_1 \left(t' - t'' \right) \right)^2 + B\beta g_1 \left(t' - t'' \right) \right] dt' dt'' / T^2 \tag{6}$$

The reduced second moment of intensity or the variance is hence

$$v_2(T) = \int_0^T \int_0^T [A\beta \left(g_1 \left(t' - t'' \right) \right)^2 + B\beta g_1 \left(t' - t'' \right)] dt' dt'' / T^2 \tag{7}$$

Since $g_1(t)$ is an even function, the double integral simplifies to

$$v_2(T) = A\beta \int_0^T 2 \left(1 - \frac{t}{T} \right) \left[g_1(t)^2 \right] \frac{dt}{T} + B\beta \int_0^T 2 \left(1 - \frac{t}{T} \right) \left[g_1(t) \right] \frac{dt}{T} \tag{8}$$

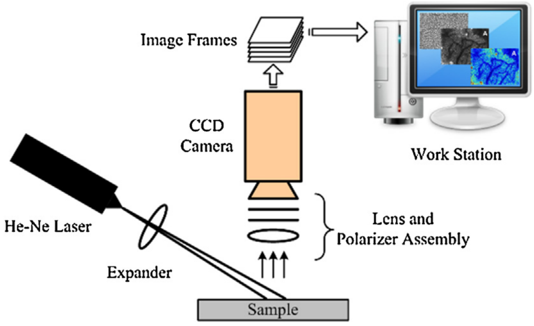

Fig. 1. Laser speckle contrast imaging system.

Assuming that the velocities of the scatterers have a Lorentzian distribution, which gives $g_1(t) = e - t/\tau_c$ and recognizing that the square root of the variance is the speckle contrast, Eq. (8) can be simplified to:

$$K(T, \tau_c) = \left[\beta\rho^2 \frac{e^{-2x} + 2x - 1}{2x^2} + 4\beta\rho(1-\rho)\frac{e^{-x} + x - 1}{x^2}\right]^{1/2} \tag{9}$$

where $x = T/\tau_c$, $\rho = I_f/\left(I_f + I_s\right)$. is the fraction of total light that is dynamically scattered,

When there are no static scatterers present, $\rho \to 1$ and Eq. (9) simplifies to Eq. (3). However, Eq. (9) is incomplete since in the opposite limit of only static scattering occurs ($\rho \to 0$), it does not reduce to a constant speckle contrast value as one would expect for spatial speckle contrast. An additional factor that has been neglected is experimental noise, which can have a significant impact on measured speckle contrast. Experimental noise can be broadly categorized into shot noise and camera noise. Shot noise is the largest contributor of noise, and it is primarily determined by the signal level at the pixels. In the light of these arguments, we can rewrite Eq. (9) as:

$$K(T, \tau_c) = \left[\beta\rho^2 \frac{e^{-2x} + 2x - 1}{2x^2} + 4\beta\rho(1-\rho)\frac{e^{-x} + x - 1}{x^2} + V_{noise}\right]^{1/2} \tag{10}$$

where V_{noise} is the constant variance due to experimental background noise. We also recognize that while V_{noise} makes the model more complete, it does not add any new information about the dynamics of the system, all of which is held in τ_c. The static speckle is determined by V_{noise}. Experiment data show that the sensitivity of image contrast to the speed difference seems to be inversely proportional to the power of the speckle contrast K_0. Based on this we make an improvement on LSI algorithm, eventually, new algorithm give different laser speckle system the capability of free from the interference of noise.

2.2. Experiment setup

Fig. 1 shows that the LSI system consists of three basic parts: laser source, image capturing device and processing center. Laser beam is expanded before illuminates on the sample. Then the backscattered light is collected by CCD camera after passing through a lens and a polarizer assembly. Finally, raw images are stored on a PC for image processing.

In the system there are several parameters that may exert great influence on image contrast, such as those present in the laser source, in the image processing part and in the image acquisition part. First, the decreasing of mono-chromaticity and polarization ratio in laser device may cause the increasing of β value of system [12]. Therefore, their characteristics and consequent influence should be taken into consideration for relative speed evaluation. Secondly, we can achieve different size of laser speckle by varying optical magnification M and clear aperture D. In the context of Nyquist sampling criterion, the increasing of speckle size may decrease accuracy of image contrast. Finally, random noise in image acquisition part affects β value. Furthermore, the selection of exposure time has a great impact on image contrast. Appropriate adjustment of exposure time can enlarge the range of linear speed response.

The laser device used was a He-Ne laser source (25-LHP-151-230, Melles Griot, USA). The monochrome camera is a 12 bit thermoelectrically cooled CCD camera (AlliedGE1050, GIGE, BC, Germany) equipped with a close-focus zoom lens (18–108 mm, f/2.5-close, Edmund Optics #52-247, Barrington, NJ, USA). The resolution was 1600 × 1200 pixels. Image acquisition from the monochrome camera was achieved with LabVIEW software and stored into PC (3.4 GHz i7 core, 4GB DDR2 memory). 30 raw images were subsequently converted in computer to contrast images.

Fig. 2 shows a flow phantom experiment which was proposed by J. C. Ramirez-San-Juan [11] to develop and validate our new algorithm. We inject a flow of animal blood liquor which. The flow path is organized such that the flow speed at point A is two times faster than at point B. Since high flow speed causes low image contrast, the difference of contrast between two points can be used to evaluate relative speed. Raw images were converted using a 7 × 7 sliding window as usually used in LSI image analysis. A comparison was made between our algorithm and other two algorithms, namely the temporal and spatial ones. Our aim was to increase the efficiency of imaging and accuracy of relative speed evaluation.

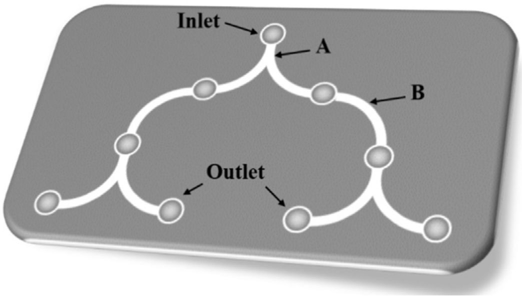

Fig. 2. Schematics of flow phantom experiment. A flow of animal blood liquor is injected in inlet port A, and then it flows to two equal branches B towards the outlet.

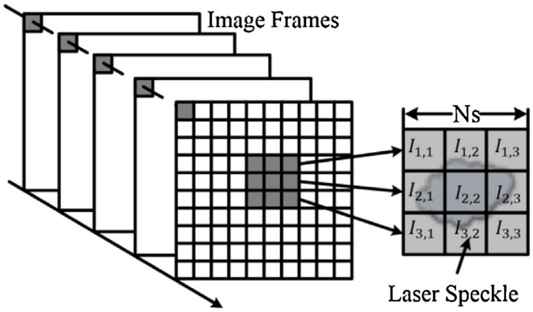

Fig. 3. Contrast imaging based on spatial and temporal algorithm. Few raw images were collected per condition, then converted to speckle contrast image using a $N_s \times Ns$ pixel sliding window. The contrast of each pixel is computed from its neighborhood pixels.

3. New algorithm and principles

3.1. Improvement of efficiency

As seen from Eq. (1), in $N_s \times N_s$ window, the power of standard deviation is

$$\sigma^2 = \frac{\{\sum_{x=1}^{N_s}\sum_{y=1}^{N_s}(I_{x,y} - \frac{1}{N_S^2}\sum_{x=1}^{N_s}\sum_{y=1}^{N_s} I_{x,y})^2\}}{N_S^2 - 1} \tag{11}$$

where x and y denote the position of contrast pixel in the observing window and $N_S^2$is the size of the window. $I_{x,y}$ is the signal intensity of pixel at coordinate (x,y) in processing unit.

We introduce the improved standard deviation σ' as:

$$\sigma' = \frac{\{\sum_{x=1}^{N_s}\sum_{y=1}^{N_s}(I_{x,y} - I_{0.5(N_s+1),0.5(N_s+1)})\}}{{N_S}^2 - 1} \tag{12}$$

which is the average of the differences between the intensity in the central pixel and the surrounding pixels (Fig. 3), which has less complexity than σ of Eq. (11), hence short time consumption [13–16].

Our main objective is to simplify the process of computation to improve efficiency. According to Nyquist sampling criterion, a larger size of the observing window for certain size of laser speckle can increase the accuracy of contrast. Consequently, we have a conflict between efficiency and accuracy. Improvements in accuracy and efficiency are the essential elements for wider application of laser speckle contrast imaging in medical diagnostics. The new algorithm we present aims at efficiency and accuracy in contrast image processing. Due to the complexity of Eq. (11), the size of the observing window affects the efficiency of processing, hence time consumption [13–16].

The new efficient approach can be described as follow:

$$C = \frac{I}{\sigma'} = \frac{\{\sum_{x=1}^{N_s}\sum_{y=1}^{N_s} I_{x,y}\}/{N_S}^2}{\{\sum_{x=1}^{N_s}\sum_{y=1}^{N_s}(I_{x,y} - I_{0.5(N_s+1),0.5(N_s+1)})\}/({N_S}^2 - 1)} \tag{13}$$

A bigger C value in Eq. (13) accounts for high flow speed, equal to lower K value in LSI algorithm. Here high speed region show as brightness in speckle contrast image.

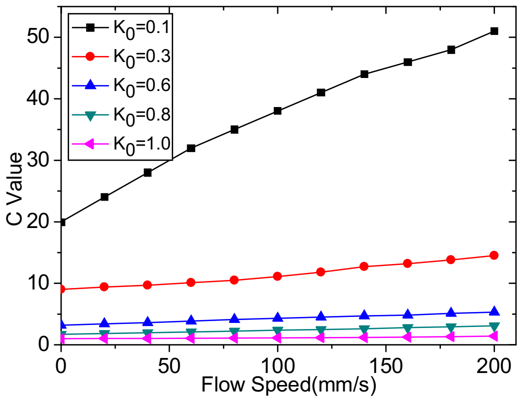

Fig. 4. Relation between the averaged C value and the speed difference as a function of the speckle contrastK_0 at point A.

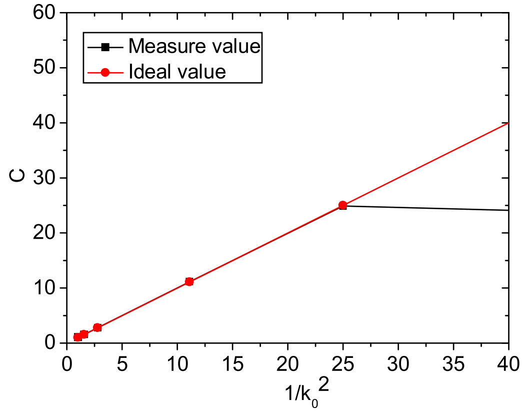

Fig. 5. Relation between the C value and the inverse power ofK_0.

Then, experimental data show the relationship between contrast and background noise. The sensitivity of the C value was inversely proportional to the power of K_0 value, K_0 being defined as the speckle contrast value under the condition of zero flow speed through Eq. (1).

3.2. Reduction of background noise

From the laser speckle contrast imaging theory, the relationship of flow speed between two different points can be derived from the relationship of image contrast between two different points. In Fig. 2, the speed at point A is twice faster as that at point B. Then, the proportional relationship between these two points was around two for all range of flow speed.

A similar trend was found for contrast in LSI, for this time C value increased as the flow speed goes high. It can also be seen from the results shown in Fig. 4 that C has a corresponding value C_0 for all cases of $K_0$where, K_0 is defined as the speckle contrast value under the condition of zero flow speed. The K_0 value can be changed by varying camera's photosensitivity (ISO).

This K_0 value was considered as the background noise V_{noise} [Eq. (10)] conducted by static speckle, which was neglected in the previous experiment [18]. The K_0 value is various in different LSI system, we must eliminate static part from dynamic for laser speckle. Furthermore, as seen from data in Fig. 5, the sensitivity of the C value seems to be inversely proportional to the power of K_0 (Eq. (1)) in the range of 0.2–0.6. Once ISO was fixed, K_0 value can be achieved by Eq. (1). Thus, the new algorithm which normalizes and eliminates the background noise for different systems, can be defined as:

$$C_{new} = (C - C_0)K_0^2 \tag{14}$$

In comparison with results shown in Fig. 4, the C_{new} value was free from the effects of the background noise for cases of $1/K_0^2$ up to 25 (K_0value is 0.2 up to 0.6) which meet contrast requirements of human skin tissue range of 0.2–0.6, displayed in Fig. 5 and Fig. 6 .

Since the new algorithm possesses lower complexity, data from an efficiency evaluation experiment of raw images processing demonstrate the potential of this new algorithm, displayed in Fig. 7. Fig. 7 shows a comparison of time consumption for four imaging algorithms in LSI analysis. As expected, increasing size of sliding window increased processing time. Spatial

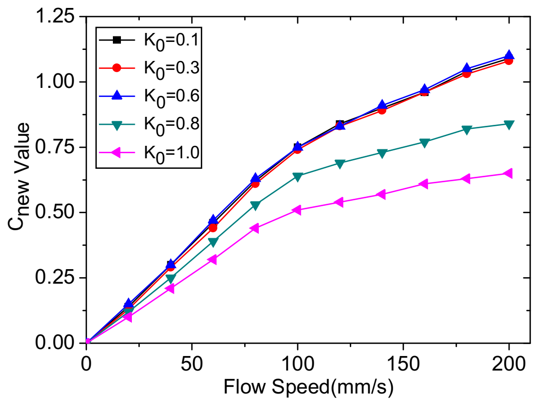

Fig. 6. Relation between the averaged C_{new} value and the speed difference as a function of the speckle contrastK_0. Compared to Fig. 5, after eliminate static part form dynamic, C_{new}value was free from effects of K_0(0.2–0.6). Thus, for different K_0(0.2–0.6) value, the result is the same corresponding to different flow speed.

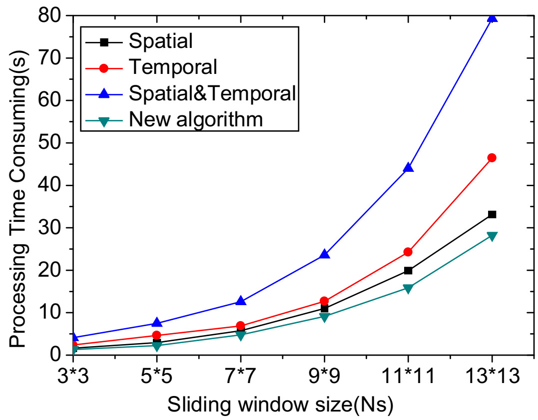

Fig. 7. Plot of time consumption in process of contrast imaging by three imaging algorithms for routinely cases of N_s. The lower complexity of the new algorithm reduces the consumption of processing time to a great extent.

and temporal algorithms exhibited higher sensitivity to the change of sliding window in comparison with our new algorithm. Due to the lower complexity of the new algorithm, almost 20.1% and 34.5% reduction in processing time can be achieved in comparison with spatial and temporal algorithms, respectively, when sliding window size is 11 × 11 pixels.

Furthermore, this new algorithm has an excellent performance versus other two algorithms at assessing the relative changes for all ranges of flow speed. From Parthasarathy's work [5] we know that the spatial algorithm is more sensitive to the static component of the scattered light, while the temporal algorithm is more sensitive to the dynamic component of the scattered light [17–19]. In clinical trials, the flow speed of blood in human skin tissue was full of variety, and so does LSI system. But our algorithm can adapt itself through eliminate static part from laser speckle based on K_0value.

In the skin phantom experiments, we selected two standard vessels for which the flow speed of vessel A was twice as that of vessel B [13]. The size of laser speckle was set to 12 pixels per speckle by Eq. (5), to satisfy the Nyquist sampling criterion [19–22].

$$D_S = 2.44\lambda\,(1 + \mathrm{M}) f_{\#} \tag{15}$$

where M is the optical magnification, $f_{\#}$ the f-stop of the imaging optics, and ¦Ë the wavelength of the laser source.

The relative flow speed V_{rel} between vessel A and B is:

$$V_{rel} = C_{new\_A} / C_{new\_B} \tag{16}$$

As seen from Fig. 8, for all range of flow speed in vessel A, results from the spatial algorithm have a decline as flow speed increase. When flow speed was low, the new algorithm and the spatial algorithm have a better accuracy due to its sensitivity to static components of scattered light. At higher speeds, the temporal and the new algorithms achieved a higher accuracy than the spatial algorithm, which is consistent with previous works [13].

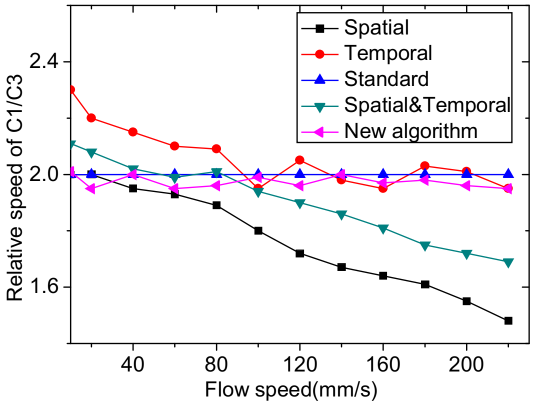

Fig. 8. The relative change of flow speed, for the spatial, temporal and new algorithm analysis, for routinely cases of flow speed. The new algorithm has a precise evaluation against others for wide range of flow speed.

4. Conclusion

We presented a new speckle imaging algorithm that has the capability to obtain speckle images over a wide range of flow speeds. We also theoretically analyzed the static part of laser speckle which was conducted by background noise.K_0 value was conducted by static speckle, this value various in different LSI system. Once system fixed, this new algorithm can eliminate static noise from laser speckle image based on K_0value. System can totally free from the interference of static noise, especially in blood flow speed evaluation experiment. Meanwhile, due to the less complexity of computation, we achieved high efficiency in laser speckle imaging. Additionally, our new algorithm has a high sensitivity to the motion of particles for all cases of flow speed. In clinical areas, the flow speed of blood in human skin tissue was full of variety, this new algorithm can adapt itself to different LSI system by eliminate static background noise. High accuracy of evaluation and high efficacy of processing can be achieved by the combination of temporal and spatial algorithm.

In conclusion, the new algorithm presented here takes temporal integration and spatial integration into consideration, normalizes and eliminates background noise for imaging systems and has a higher efficiency and wider applicability.

Acknowledgements

This work has been Supported by the Innovation Program of Shanghai Municipal Education Commission (15ZZ072).

Reference:

[1] A. Fercher, J. Briers, Flow visualization by means of single-exposure speckle photography, Opt. Commun. 37 (5) (1981) 326–330.
[2] A.K. Dunn, Laser speckle contrast imaging of cerebral blood flow, Ann. Biomed. Eng. 40 (2) (2012) 367–377.
[3] J. Goodman, Speckle Phenomena in Optics: Theory and Application, Roberts & Company, 2007.
[4] A. Rege, Anisotropic processing of laser speckle images improves spatiotemporal resolution, Biomed. Eng. 59 (5) (2012) 1272–1280.
[5] B. Parthasarathy, J. Tom, A. Gopal, X. Zhang, K. Dunn, Robust flow measurement with multi-exposure speckle imagin, Opt. Express 16 (3) (2008) 1975–1989.
[6] A. Mazhar, T.B. Rice, Laser speckle imaging in the spatial frequency domain, Biomed. Opt. Express 2 (6) (2011) 1553–1563.
[7] S. Liu, P. Li, Q. Luo, Fast blood flow visualization of high resolution laser speckle imaging data using graphics processing unit, Opt. Express 16 (2008) 14321–14329.
[8] T.M. Le, New insights into image processing of cortical blood flow monitors using laser speckle imaging, Med. Imaging 26 (6) (2007) 833–842.
[9] O. Yang, D. Cuccia, B. Choi, Real-time blood flow visualization using the graphics processing unit, J. Biomed. Opt. 16 (1) (2011) 016009–016014.
[10] D.A. Boas, A.K. Dunn, Laser speckle contrast imaging in biomedical optics, J. Biomed. Opt 15 (1) (2010) 011109.
[11] R. Bandyopadhyay, A.S. Gittings, S.S. Suh, P.K. Dixon, D.J. Durian, Speckle-visibility spectroscopy: a tool to study time-varying dynamics, Rev. Sci. Instrum. 76 (1) (2005) 093110.
[12] O. Thompson, M. Andrews, E. Hirst, Correction for spatial averaging in laser speckle contrast analysis, Biomed Opt. Express 2 (4) (2011) 1021–1029.
[13] J.C. Ramirez-San-Juan, E. Mendez-Aguilar, N. Salazar-Hermenegildo, A. Fuentes-Garcia, R. Ramos-Garcia, B. Choi, Effects of speckle/pixel size ratio on temporal and spatial speckle-contrast analysis of dynamic scattering systems: implications for measurements of blood-flow dynamics, Biomed. Opt. Express 4 (10) (2013) 1883–1889.
[14] G.A. Armitage, K.G. Todd, A. Shuaib, I.R. Winship, Laser speckle contrast imaging of collateral blood flow during acute ischemic stroke, J. Cereb. Blood Flow. Metab. 30 (8) (2010) 1432–1436.
[15] C. Bordier, C. Andraud, E. Charron, J. Lafait, M. Anastasiadou, Illustration of a bimodal system in intralipid-20% by polarized light scattering: experiments and modeling, Appl. Phys. A 94 (4) (2009) 347–355.
[16] J.D. Briers, S. Webster, Laser speckle contrast analysis (LASCA): a nonscanning, full-field technique for monitoring capillary blood flow, J. Biomed. Opt. 1 (2) (1996) 174–179.
[17] P. Zakharov, A.C. Volker, M.T. Wyss, F. Haiss, N. Calcinaghi, C. Zunzunegui, A. Buck, F. Scheffold, B. Weber, Dynamic laser speckle imaging of cerebral blood flow, Opt. Express 17 (16) (2009) 13904.
[18] L.P. Song, Effect of signal intensity and camera quantization on laser speckle contrast analysis, Biomed. Opt. Express 4 (1) (2013) 89–104.
[19] S.M. Daly, 'Go with the flow': a review of methods and advancements in blood flow imaging, J. Biophoton. 6 (3) (2013) 217–255.
[20] H.Y. Cheng, Modified laser speckle imaging method with improved spatial resolution, J. Biomed. Opt. 8 (3) (2003) 559–564.

[21] S.S. Liu, Fast blood flow visualization of high-resolution laser speckle imaging data using graphics processing unit, Opt. Express 16 (19) (2008) 14321–14329.
[22] H. Yang, R. Li, P. Kong, Q.C. Sun, M.J. Biggs, V. Zivkovic, Avalanche dynamics of granular materials under the slumping regime in a rotating drum as revealed by speckle visibility spectroscopy, Phys. Rev. E 91 (4) (2015) 042206 (8).